

# Synthesis of High Surface Area Phosphosilicate Glasses by a Modified Sol–Gel Method

Antonio Aronne,<sup>\*,†</sup> Maria Turco,<sup>‡</sup> Giovanni Bagnasco,<sup>‡</sup> Pasquale Pernice,<sup>†</sup>  
Martino Di Serio,<sup>§</sup> Nigel J. Clayden,<sup>||</sup> Elisa Marenna,<sup>†</sup> and Esther Fanelli<sup>†</sup>

Department of Materials and Production Engineering, University of Naples Federico II,  
Piazzale Tecchio, 80125, Naples, Italy, Department of Chemical Engineering, University of Naples  
Federico II, Piazzale Tecchio, 80125, Naples, Italy, Department of Chemistry, University of Naples  
Federico II, Via Cinthia, 80125, Naples, Italy, and School of Chemical Science and Pharmacy,  
University of East Anglia, Norwich NR4 7TJ

Received December 20, 2004

High surface area phosphosilicate glasses were synthesized by a new sol–gel method and characterized for structural, textural, and acid properties by X-ray diffraction, thermogravimetry/differential thermal analysis, IR spectroscopy (Fourier transform and diffuse reflectance Fourier transform), solid state <sup>31</sup>P and <sup>29</sup>Si NMR spectroscopy, N<sub>2</sub> adsorption, and NH<sub>3</sub> temperature programmed desorption. The glasses were synthesized by a sol–gel route hydrolyzing the precursors in an almost solely aqueous environment. Microstructural changes occurring during the conversion of the gels into the corresponding glasses were investigated. For all dried gels (383 K), the elimination of organic residues was complete at 673 K. After this heat treatment, ca. 80% of the phosphorus was present as free phosphoric acid except for the sample with the highest P content for which the percentage dropped to ca. 47%. Textural properties of samples treated at 673 K were greatly influenced by the composition. Surface area decreased and pore dimension increased with increasing phosphorus content, indicating a gradual transformation of the siloxane matrix from microporous to mesoporous. Brønsted acid sites of differing strength, mainly related to the presence of phosphoric acids, were found. The surface concentration and strength of acid sites increased with phosphorus content.

## Introduction

Amorphous and crystalline phosphosilicates exhibit interesting technological and structural properties. Gel-derived phosphosilicate glasses find applications as fast proton conductors<sup>1–6</sup> and are potential bioactive materials<sup>7–9</sup> after the appropriate chemical modification. In addition, liquid or glassy phosphoric acid supported on silicon phosphate phases has been used as a solid acid catalyst for olefin oligomerization and hydration.<sup>10–11</sup> Interestingly, in some crystalline

phases as well as in phosphosilicate glasses the Si<sup>4+</sup> ions can assume the unusual octahedral coordination.<sup>12–15</sup>

The sol–gel chemistry of phosphosilicates has been extensively studied.<sup>16–19</sup> It has been shown that the choice of the phosphorus molecular precursor plays a fundamental role in determining the characteristics of the final product, such as the extent of copolymerization between silicate and phosphate units, the type of crystalline phases and their relative amount, the actual phosphorus content, and textural and surface properties. Livage et al.<sup>16</sup> showed that phosphate esters, PO(OR)<sub>3</sub>, react too slowly with water at ambient conditions in comparison with tetraethoxy silane, whereas orthophosphoric acid reacts too fast during the polycondensation reaction leading to precipitation rather than gelation. More convenient precursors can be obtained either by dissolving P<sub>2</sub>O<sub>5</sub> in alcohols forming different PO(OH)<sub>3–x</sub>(OR)<sub>x</sub> species with chemical reactivity intermediate between

\* To whom correspondence should be addressed. Tel: +39 081 76 82556. Fax: +39 081 76 82595. E-mail: anaronne@unina.it.

<sup>†</sup> Department of Materials and Production Engineering, University of Naples Federico II.

<sup>‡</sup> Department of Chemical Engineering, University of Naples Federico II.

<sup>§</sup> Department of Chemistry, University of Naples Federico II.

<sup>||</sup> University of East Anglia.

- (1) Nogami, M.; Daiko, Y.; Goto, Y.; Usui, Y.; Kasuga, T. *J. Sol-Gel Sci. Technol.* **2003**, *26*, 1041.
- (2) Daiko, Y.; Kasuga, T.; Nogami, M. *Chem. Mater.* **2002**, *14*, 4624.
- (3) Matsuda, A.; Kanzaki, T.; Tadanaga, K.; Tatsumisago, M.; Minami, T. *Solid State Ionics* **2002**, *154–155*, 687.
- (4) Aparicio, M.; Klein, L. C. *J. Sol-Gel Sci. Technol.* **2003**, *28*, 199.
- (5) D'Apuzzo, M.; Aronne, A.; Esposito, S.; Pernice, P. *J. Sol-Gel Sci. Technol.* **2000**, *17*, 247.
- (6) Clayden, N. J.; Esposito, S.; Pernice, P.; Aronne, A. *J. Mater. Chem.* **2002**, *12*, 3746.
- (7) Saravanapavan, P.; Jones, J. R.; Pryce, R. S.; Hench, L. L. *J. Biomed. Mater. Res., Part A* **2003**, *66A*, 110.
- (8) Roman, J.; Padilla, S.; Vallet-Regí, M. *Chem. Mater.* **2003**, *15*, 798.
- (9) Cerruti, M.; Magnacca, G.; Bolis, V.; Morterra, C. *J. Mater. Chem.* **2003**, *13*, 1279.
- (10) Krawietz, T. R.; Lin, P.; Lotterhos, K. E.; Torres, P. D.; Barich, D. H.; Clearfield, A.; Haw, J. F. *J. Am. Chem. Soc.* **1998**, *120*, 8502.
- (11) Fougret, C. M.; Hölderich, W. F. *Appl. Catal., A* **2001**, *207*, 295.

- (12) Weeding, T. L.; de Jong, B. H. W. S.; Veeman, W. S.; Aitken, B. G. *Nature* **1985**, *318*, 352.
- (13) Makart, H. *Helv. Chim. Acta* **1967**, *50*, 399.
- (14) Dupree, R.; Holland, D.; Mortuza, M. G. *Nature* **1987**, *328*, 416.
- (15) Nogami, M.; Miyamura, K.; Kawasaki, Y.; Abe, Y. *J. Non-Cryst. Solids* **1997**, *211*, 208.
- (16) Livage, J.; Barboux, P.; Vandenborre, M. T.; Schmutz, C.; Taulelle, F. *J. Non-Cryst. Solids* **1992**, *147 and 148*, 18.
- (17) Tian, F.; Pan, L.; Wu, X. *J. Non-Cryst. Solids* **1988**, *104*, 129.
- (18) Szu, S.-P.; Klein, L. C.; Greenblatt, M. *J. Non-Cryst. Solids* **1992**, *143*, 21.
- (19) Fernández-Lorenzo, C.; Esquivias, L.; Barboux, P.; Maquet, J.; Taulelle, F. *J. Non-Cryst. Solids* **1994**, *176*, 189.

PO(OR)<sub>3</sub> and PO(OH)<sub>3</sub> or by using phosphoryl chloride.<sup>16</sup> P—O—Si or P—O—P linkages were not observed in the sol or in the dried gels but only in the heat-treated gels using PO(OC<sub>2</sub>H<sub>5</sub>)<sub>3</sub>,<sup>17–19</sup> PO(OH)<sub>3</sub>,<sup>18,19</sup> and P(OCH<sub>3</sub>)<sub>3</sub><sup>18</sup> as phosphorus precursors. The extent of cross linking is also affected by the phosphorus content. Clayden et al.<sup>20</sup> studied phosphosilicate gels with two different P<sub>2</sub>O<sub>5</sub> content levels (10 and 30 mol %) synthesized from POCl<sub>3</sub>. They found that both dried gels (373 K) contained siloxane frameworks and trapped isolated molecules of orthophosphoric acid. After they were heated at 673 K, the samples exhibit different behaviors. In the material with a low phosphorus content, the predominant reaction was partial dehydroxylation of silanol groups, while in that with a high phosphorus content, cross linking of the phosphorus and siloxane network took place. After treatment at higher temperatures, P—O—Si bonds were also formed in the sample with lower phosphorus content. On the other hand, crystallization of Si<sub>5</sub>O(PO<sub>4</sub>)<sub>6</sub> occurred at 673 K only in the 30 mol % P<sub>2</sub>O<sub>5</sub> sample, while the other sample keeps its amorphous nature up to 1273 K. Kim and Tressler,<sup>21</sup> using PO(OH)<sub>3</sub> as a precursor, found that Si<sub>3</sub>(PO<sub>4</sub>)<sub>4</sub> crystallized at about 573 K and SiP<sub>2</sub>O<sub>7</sub> at about 1073 K in phosphosilicate gels containing 56 mol % of P<sub>2</sub>O<sub>5</sub>. On the other hand, Cao et al.,<sup>22</sup> using P<sub>2</sub>O<sub>5</sub> as precursor, observed the formation of the crystalline phase Si<sub>5</sub>O(PO<sub>4</sub>)<sub>6</sub> at a temperature higher than 573 K, independently of the starting gel composition.

The characterization of textural and surface properties of these materials is important in view of their use as catalysts or sensors. Very different values for the specific surface areas of gel-derived phosphosilicate glasses have been reported in the literature. Kim and Tressler<sup>21</sup> found specific surface areas lower than 4 m<sup>2</sup> g<sup>−1</sup> for gel-derived glasses with nominal P<sub>2</sub>O<sub>5</sub> content of 56 mol %, while Massiot et al.<sup>23</sup> found values lower than 16 m<sup>2</sup> g<sup>−1</sup> for a nominal P<sub>2</sub>O<sub>5</sub> content of 33 mol %. On the other hand, Daiko et al.<sup>2</sup> reported that the surface areas of gel-derived glasses with nominal P<sub>2</sub>O<sub>5</sub> content of 5 mol %, heated to 873 K, were affected by the phosphorus precursor, PO(OCH<sub>3</sub>)<sub>3</sub> or POCl<sub>3</sub>. Such an effect might also be related to difference in the actual P<sub>2</sub>O<sub>5</sub> content, since the type of precursor strongly influences the composition.

In the present paper, phosphosilicate gel-derived glasses, prepared by a new synthetic procedure, are studied. In particular, the possibility of hydrolyzing the organometallic precursors in an almost solely aqueous environment is explored. This method may facilitate the introduction of hydrosoluble inorganic precursors into the synthesis medium. As shown later, this method also allows high surface area phosphosilicate glasses to be obtained. The structural changes induced by the thermal treatment of the gel as well as the surface acidic properties of the gel-derived glasses are also investigated.

## Experimental Section

Phosphosilicate glasses, the nominal composition of which can be expressed by the formula  $x\text{P}_2\text{O}_5 \cdot (100 - x)\text{SiO}_2$ , with  $x = 5$  (5P), 10 (10P), 20 (20P), and 30 (30P), were prepared by a sol–gel method using phosphoryl chloride, POCl<sub>3</sub> (99%, Aldrich Chemical), and tetraethoxysilane, Si(OC<sub>2</sub>H<sub>5</sub>)<sub>4</sub> (99%, Gelest) (TEOS), as starting materials.

TEOS was hydrolyzed for 1 h at 323 K without any alcoholic solvent using hydrochloric acid as catalyst. The molar ratio employed was TEOS:H<sub>2</sub>O:HCl = 1:20:0.01. This solution was allowed to cool to room temperature, after which it was mixed with a solution of POCl<sub>3</sub> in anhydrous ethanol (EtOH) having a molar ratio POCl<sub>3</sub>:EtOH = 1:6 and left stirring. A transparent gel was obtained from this final solution with gelation occurring after 48, 36, 24, and 12 h for 5P, 10P, 20P, and 30P samples, respectively, showing that increasing the phosphorus content in the gel composition leads to shorter gelation times. The gelled systems were held for 2 days at room temperature before drying. The gels were fully dried in air at 383 K in an electric oven for 3 days. After these treatments, transparent and amorphous xerogels were obtained for all compositions.

Silica gel derived glass was also synthesized hydrolyzing TEOS in the conditions described above. In this case, gelation was observed after 48 h at room temperature.

The phosphorus and silicon contents in the gel derived glasses were determined by ion chromatography and spectrophotometry, after dissolving powdered samples, slowly preheated up to 1273 K, in HF solutions, according to standard procedures.<sup>24–27</sup>

Phosphorus was determined as phosphate ion using a Metrohm IC761 Ion Chromatograph equipped with conductivity detector. The reproducibility of phosphate concentration for a particular sample was in the range 0.2–1.0%, depending on the absolute phosphate content. The average recoveries were in the range 98.9–101.5%. Additionally, the phosphate content in the studied samples was also checked with an independent method of analysis based on spectrophotometric determination. Actually, molybdophosphoric acid was formed and reduced by stannous chloride to intensely colored molybdenum blue. The phosphate concentration was proportional to the absorbance at 690 nm. Differences between the two methods were lower than the experimental uncertainty.

Silicon content was determined by spectrophotometric method. Ammonium molybdate at a pH of approximately 1.2 reacts with silica and with any phosphate present to produce heteropoly acids. The interference of phosphate was avoided by adding oxalic acid that destroys the molybdophosphoric acid but not the molybdosilicic one. The concentration of the “molybdate-reactive” silica was proportional to the absorbance at 410 nm.

Thermogravimetric/differential thermal analysis (TG/DTA) analyses were carried out by using a Netzsch simultaneous thermoanalyzer STA 409C with Al<sub>2</sub>O<sub>3</sub> as reference material. The STA curves, recorded in air from room temperature up to 1273 K at a heating rate of 10 K min<sup>−1</sup>, were carried out on 50 mg of the dried gels.

The amorphous nature of the dried gels as well as the nature of the crystallizing phases was ascertained by X-ray diffraction using a Philips diffractometer model PW1710 (Cu Kα) with a scan rate of 1° min<sup>−1</sup>.

- (20) Clayden, N. J.; Esposito, S.; Pernice, P.; Aronne, A. *J. Mater. Chem.* **2001**, *11*, 936.
- (21) Kim, Y. S.; Tressler, R. E. *J. Mater. Sci.* **1994**, *29*, 2531.
- (22) Cao, Z.; Lee, B. I.; Samuels, W. D.; Wang, L. Q.; Exarhos, G. J. *J. Mater. Res.* **1998**, *13*, 1553.
- (23) Massiot, Ph.; Centeno, M. A.; Carrizosa, I.; Odriozola, J. A. *J. Non-Cryst. Solids* **2001**, *292*, 158.

- (24) Weiss, J. *Ion Chromatography*; VCH: Weinheim, 1995.
- (25) Chalmers, R. A. *Standards and Standardization in Chemical Analysis in Wilson and Wilson's Comprehensive Analytical Chemistry*; Svehla, G., Ed.; Elsevier: Amsterdam, 1975; Vol. III.
- (26) *Official Methods of Analysis of the AOAC*, 17th ed.; Horwitz, W., Ed.; Gaithersburg, 2000.
- (27) *Standard Methods for the Examination of Water and Wastewater*, 20th ed.; APHA AWWA WEF: Washington, 1998.

Fourier transform (FT) IR spectra of dried and heat-treated gel samples were carried out at room temperature by a Nicolet system, Nexus model, equipped with a DTGS KBr (deuterated triglycine sulfate with potassium bromide windows) detector. The absorption spectra were recorded in the 4000–400-cm<sup>-1</sup> range with a spectral resolution of 2 cm<sup>-1</sup> on samples diluted in KBr. The spectrum of each sample represents an average of 64 scans, which were corrected for the spectrum of the blank KBr. To allow the comparison of the absorbance values, all FTIR spectra have been normalized with respect to the maximum absorbance value recorded for each spectrum.

Diffuse reflectance Fourier transform (DRIFT) IR spectra were recorded at room temperature using the above spectrometer equipped with a SpectraTech diffuse reflectance sample cell. Samples were previously diluted in KBr (2 wt %), and 64 scans were collected with a resolution of 2 cm<sup>-1</sup>. The spectra, corrected for KBr, are reported in Kubelka–Munk units.

Solid-state <sup>29</sup>Si and <sup>31</sup>P NMR spectra were acquired on a Bruker MSL-200 NMR spectrometer operating at 39.73 and 81.0 MHz, respectively. Magic-angle sample spinning (MAS) was carried out using a Bruker double-bearing rotor system with 7-mm zirconia rotors. Typical spinning speeds were 4–5 kHz, which was sufficient to make the spinning sidebands of low intensity and outside the region of interest. The choice of recycle delay was based on previous literature values together with the results obtained in control experiments with recycle delays of 10, 100, and 300 s for <sup>31</sup>P and 60, 180, and 300 s for <sup>29</sup>Si. For the <sup>31</sup>P MAS NMR, a 90° pulse of 5 μs together with a recycle delay of 300 s was used over a spectral width of 40 kHz. Transients (280) were collected. <sup>29</sup>Si NMR data were collected using a 45° pulse of 3-μs duration together with a recycle delay of 60 s over a spectral width of 20 kHz. The choice of recycle delay was based on previous literature values together with the results obtained in the above control experiments. Typically 1000 transients were acquired. All spectra were acquired with fully loaded rotors. The <sup>31</sup>P chemical shifts were referenced using the secondary reference γ-zirconium phosphate taking the more shielded resonance as -9.7 ppm with respect to 85% phosphoric acid. The siloxane Q<sub>8</sub>M<sub>8</sub> was used as a <sup>29</sup>Si secondary reference taking the M-type resonance as +11.5 ppm.

N<sub>2</sub> adsorption–desorption isotherms at 77 K were carried out by a Carlo Erba-Fisher apparatus model 1990. The sample was previously treated in the sample cell at 443 K under vacuum up to complete degassing. Then constant amounts of N<sub>2</sub> (8 cm<sup>3</sup> at STP) were automatically introduced up to saturation. Desorption of N<sub>2</sub> was carried out stepwise by constant volume drawings (4 cm<sup>3</sup> at 307 K and at each equilibrium pressure). From the measured pressure values, the amounts of N<sub>2</sub> retained by the sample at each adsorption or desorption step were calculated. The N<sub>2</sub> adsorption–desorption isotherms were elaborated by the Brunauer–Emmett–Teller (BET) method for the calculation of the surface areas.<sup>28</sup> The α-plot method was also employed for the calculation of the surface areas and micropore volumes.<sup>28</sup> Pore volumes were determined from the amounts of adsorbed N<sub>2</sub> at P/P<sup>0</sup> = 0.98 (desorption curve), assuming the presence of liquid N<sub>2</sub> (density = 0.807 g cm<sup>-3</sup>) in the pores under these conditions. Ammonia temperature-programmed desorption (TPD) measurements were carried out in a flow apparatus equipped with pure NH<sub>3</sub> and He lines regulated by electronic devices and a thermal conductivity detector (TCD). The sample, previously heated at 673 K in He flow for 1 h, was saturated with NH<sub>3</sub> by flowing a 1% NH<sub>3</sub>/He mixture at room temperature. After the sample was purged in a He flow to eliminate loosely bonded NH<sub>3</sub>, it was heated at a constant rate of 10 K min<sup>-1</sup> up to

**Table 1. Chemical Analysis for Gel-Derived Phosphosilicate Glasses Heated at 1273 K**

sample	nominal composition (mol %)			analyzed composition (mol %)		
	P <sub>2</sub> O <sub>5</sub>	SiO <sub>2</sub>	P/Si	P <sub>2</sub> O <sub>5</sub>	SiO <sub>2</sub>	P/Si
5P	5	95	0.105	5.00	95.0	0.105
10P	10	90	0.222	8.40	91.6	0.183
20P	20	80	0.500	11.9	88.1	0.270
30P	30	70	0.857	19.1	80.9	0.472

873 K in the He flow (30 cm<sup>3</sup> min<sup>-1</sup>). The concentration of NH<sub>3</sub> evolved from the sample during heating was continuously measured by the TCD. A PC was employed for acquiring and elaborating the TCD signal. Water that might be eventually released by the sample was eliminated by a KOH trap to avoid interference with the NH<sub>3</sub> measurement.

## Results and Discussion

### Gel Synthesis and Structural Characterization.

Gels were prepared by a new procedure, different from that previously reported<sup>5</sup> using Si(OC<sub>2</sub>H<sub>5</sub>)<sub>4</sub> and POCl<sub>3</sub> as molecular precursors. In this case, the hydrolysis of TEOS was performed in a solely aqueous acid environment using a H<sub>2</sub>O:TEOS molar ratio equal to 20:1 at 323 K. At this temperature, the hydrolysis of the TEOS led initially to partially hydrolyzed species, Si(OC<sub>2</sub>H<sub>5</sub>)<sub>4-x</sub>(OH)<sub>x</sub>, which are water soluble. As the concentration of these species increased, the initially biphasic system was transformed into a clear solution after about 1 h. Once this solution had cooled to room temperature, the alcoholic solution containing the partially substituted phosphoryl chloride species, POCl<sub>3-x</sub>(OEt)<sub>x</sub>, was slowly added, with stirring, leading to the formation of transparent homogeneous gels for each composition. Shorter gelation times were found for the present 10P and 30P gels than for the corresponding gels obtained from the hydrolysis of the TEOS in an alcoholic solution.<sup>5</sup> The different behaviors can be explained principally by the higher H<sub>2</sub>O/TEOS molar ratio though the absence of alcohol as the hydrolysis medium will also play a part. In fact, the high molar ratio will allow a faster TEOS hydrolysis leading to a higher number of oligomeric species with terminal silanol groups, so making the polycondensation reactions faster.<sup>29</sup> Under these conditions, cross condensation will not be favored as the P–O bonds are more sensitive toward hydrolysis<sup>5,20</sup> than the Si–O ones. Thus the polycondensation reactions should produce siloxane clusters containing the hydrolysis products of the POCl<sub>3-x</sub>(OEt)<sub>x</sub> species. In this case, owing to the great availability of water, molecules of ortho- and pyrophosphoric acid should be formed, a view supported by a number of NMR studies on dried phosphosilicate gels.<sup>10,30–31</sup>

The results of the chemical analyses performed on the gel-derived samples heated at 2 K min<sup>-1</sup> in an electric oven up to 1273 K are reported in Table 1. For the 5P sample, the actual composition agrees with the nominal one while differences are found for the other samples that increase with the phosphorus content. These results show that the current synthetic procedure, in comparison with the previous pro-

(28) Gregg, S. J.; Sing, K. S. W. *Adsorption, Surface Area and Porosity*; Academic Press: London, 1967.

(29) Brinker, C. J.; Scherer, S. W. *Sol–Gel Science*; Academic Press: New York, 1990.

(30) Morrow, B. A.; Lang, S. J.; Gay, I. D. *Langmuir* **1994**, *10*, 756.

(31) Kohli, P.; Blanchard, G. J. *Langmuir* **2000**, *16*, 695.



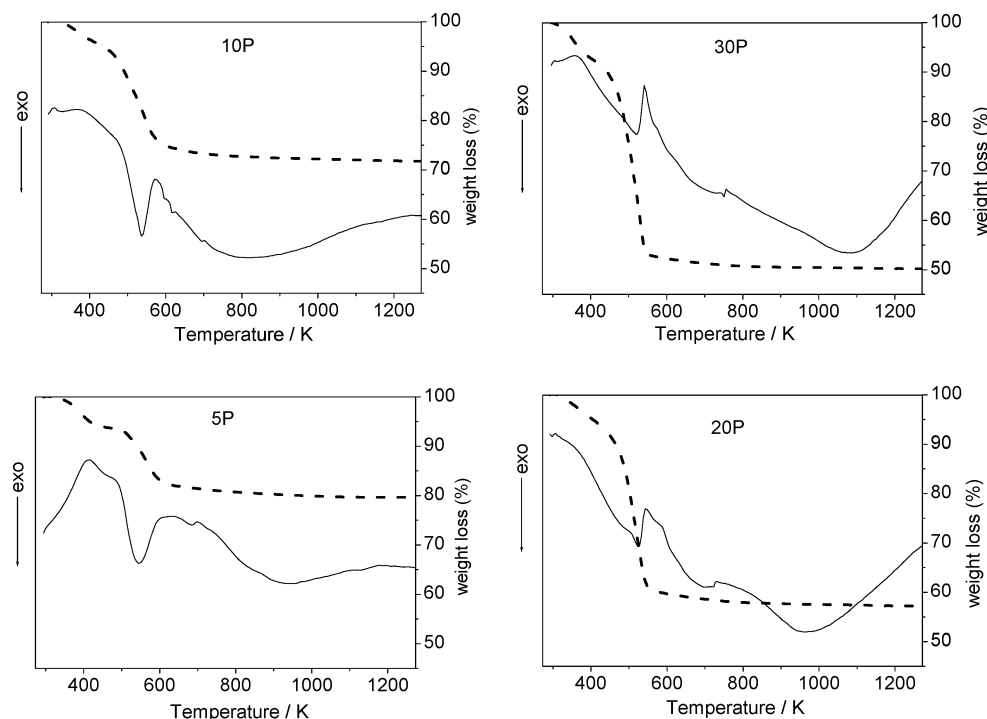


**Figure 1.** DTA (solid line)–TG (dashed line) curves of the dried gels recorded in air at 10 K min<sup>−1</sup>.

cedure,<sup>6</sup> enhances the phosphorus loss in the gel-derived glasses with a P<sub>2</sub>O<sub>5</sub> content higher than 20 mol %. Such an observation is not unusual, a similar trend for the analyzed phosphorus compositions was found by Fernández-Lorenzo et al.<sup>19</sup> Indeed, they reported that the phosphorus loss in gel-derived glasses (1223 K) of similar compositions increased not only with the P<sub>2</sub>O<sub>5</sub> content but also with the H<sub>2</sub>O/Si molar ratio.<sup>19</sup> Likewise, Szu et al.<sup>18</sup> reported that the phosphorus loss in gel-derived glasses (1073 K), synthesized starting from the same phosphorus precursor, increased with the P<sub>2</sub>O<sub>5</sub> content.

Figure 1 shows the TG/DTA curves of the dried gels recorded in air at 10 K min<sup>−1</sup>. The total weight losses given by the TG curves were 20 (5P), 28 (10P), 43 (20P), and 50 wt % (30P). In each case, the majority of the weight loss is associated with two poorly separated thermal effects seen in the corresponding DTA curves: an endothermic hump, from room temperature to about 393 K, followed by a broad exothermic peak from about 473 to 573 K. In contrast to the other gels, the DTA peaks for 5P gel are separated and take place at somewhat higher temperatures. The low-temperature peak is related<sup>4,5</sup> to evaporation from open pores of water and alcohol physically trapped in the gels, while the high-temperature one arises from burning<sup>4,5</sup> of residual organic groups in the gels. For all gels, the largest weight loss, which increases with phosphorus content, occurs below 673 K. The correlation between the weight loss and phosphorus content suggests that the intermediate organic compounds originating in the dehydration process of the gel samples are mainly related to the decomposition of species obtained from the polycondensation of the phosphorus molecular precursor (POCl<sub>3</sub> alcoholic solution).<sup>32</sup> In any

event, even evaporation of a fully hydrolyzed phosphorus species cannot be ruled out simply on the basis of the results of the chemical analysis. At temperatures higher than 673 K, no additional peaks are observed in any of the DTA curves and, concurrently, only a slight drift of the weight loss (about 1 wt %) occurs on the TG curves, indicating that the elimination of organic residues as well as of any volatile species is almost completed at 673 K.

The structural evolution of dried gels into gel-derived glasses upon heat treatment was studied by IR spectroscopy and powder XRD with a range of temperatures being used, starting from the dried gel and including gels heated to 573, 673, 973, 1273, and 1473 K. In each case, the sample was prepared by slow heating at 2 K min<sup>−1</sup> to the required temperature followed by quenching. Additionally, the 673 K samples were held at this temperature for 1 h. As ascertained by XRD analysis, the 5P and 10P gels kept their amorphous nature up to 1473 K whereas crystallization of 5SiO<sub>2</sub>·3P<sub>2</sub>O<sub>5</sub> (JCPDS card 40-457)<sup>20</sup> was observed in the 973–1273 K range for the 30P gel samples and in the early stages at 973 K for the 20P gel sample, Figure 2. However, despite this crystallization, all the gel-derived glasses heated to 1473 K were amorphous. Of note, the 30P gel previously studied showed a wider crystallization range (673–1273 K).<sup>5</sup> This difference can be related both to the actual composition of the 30P sample and to the different distribution of phosphorus atoms on the atomic scale obtained using a different synthetic procedure. Thus, the formation of a nucleation site requires a Si:P molar ratio of ~1:1 in the local gel composition. In this case, although the actual Si:P molar ratio of ~2:1 is far from the stoichiometric one, locally the amount of phosphorus must be sufficient to satisfy the stoichiometry of the crystal at a low temperature. In the present case, this condition is only met at a higher temperature, indicating that the phosphorus atoms must diffuse

(32) Massiot, Ph.; Centeno, M. A.; Gouriou, M.; Domínguez, M. I.; Odriozola, J. A. *J. Mater. Chem.* **2003**, *13*, 67.

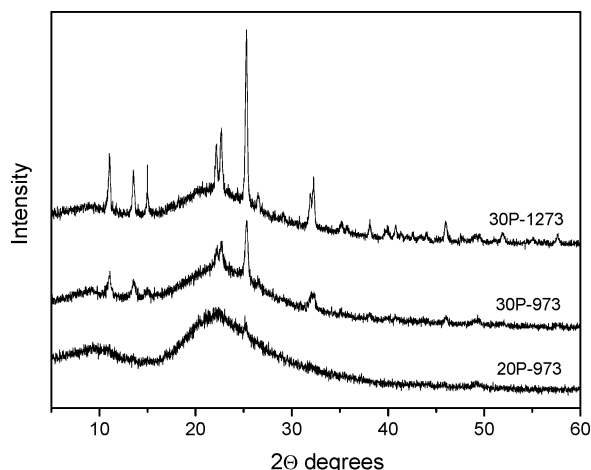


Figure 2. XRD patterns of the heat-treated gel samples.

further for the required local composition: this could be due to more homogeneous dispersion of phosphorus in the pores of the siloxane network.

FTIR spectra of dried gels and heat-treated samples are shown in Figure 3. The FTIR spectra of dried gels show the main envelope in the 1000–1300-cm<sup>-1</sup> region, where some of the vibration modes of partially hydrolyzed TEOS molecules (1168 and 1082 cm<sup>-1</sup>)<sup>33</sup> overlap the ones typical of a siloxane network (1080 and 1250 cm<sup>-1</sup>)<sup>34,35</sup> as well as the stretching modes of the (PO<sub>4</sub>)<sup>3-</sup> (980–1020 cm<sup>-1</sup>)<sup>36,37</sup> and (O<sub>1/2</sub>PO<sub>3</sub>)<sup>2-</sup> (1080–1160 cm<sup>-1</sup> and 1020–1030 cm<sup>-1</sup>)<sup>36</sup> groups. Absorption bands at 460 cm<sup>-1</sup> (Si–O–Si bending vibrations),<sup>33</sup> 800 cm<sup>-1</sup> (P–O–P and Si–O–Si symmetric stretching),<sup>33,36</sup> 970 cm<sup>-1</sup> (stretching of Si–OH bonds),<sup>35</sup> and 1650 cm<sup>-1</sup> (deformation modes of O–H bonds and of molecularly adsorbed water)<sup>5,9</sup> are also seen. Moreover, all dried gels exhibit a broad absorption band in the 3000–3750-cm<sup>-1</sup> range (stretching of O–H bonds)<sup>5,9,33</sup> with shoulders at 3230 and 3650 cm<sup>-1</sup>. These features are clearly displayed in Figure 4, where the FTIR spectra of the dried gels in the 2000–4000-cm<sup>-1</sup> wavenumber range are shown. The shoulder at 3650 cm<sup>-1</sup> is related to free Si–OH groups,<sup>9,33,38</sup> while the broad absorption band arises from SiO–H and PO–H group stretches involved in hydrogen bonding. Hydrogen bonding causes low-frequency shifts, the magnitude of which are related to the strength of hydrogen bonds in which the OH groups are involved.<sup>6,9,37</sup> When the phosphorus content increases, the intensity of the O–H band, including the component at 3650 cm<sup>-1</sup>, decreases and, at the same time, the maximum shifts to a lower frequency while the intensity of the shoulder at 3230 cm<sup>-1</sup> increases. This indicates that the number of free and weakly H-bonded silanol groups diminishes, while PO–H groups are involved in stronger H bonding. The low-intensity band at about 2990 cm<sup>-1</sup>, that appears enhanced with the phosphorus content, can be

assigned to the stretching mode of C–H bond in an aldehydic group.<sup>5</sup> The varying amount of these molecules, produced by the partial oxidation of ethanol during the dehydration of the gel samples, agrees well with the above interpretation of the trend of the weight loss found for the studied gels. Thus, in summary, the dried gels can be described as a siloxane framework containing water, unreacted molecules of precursors, residual organic molecules, and isolated silanol groups and molecules of ortho- and pyro-phosphoric acid.

The structural evolution of dried gels on heating can be followed through the absorption bands characteristic of a mixed framework of SiO<sub>4</sub> and PO<sub>4</sub> tetrahedra: 1330 cm<sup>-1</sup> (P=O bond stretch),<sup>5,39</sup> shoulder at about 1250 cm<sup>-1</sup> (Si–O bond stretch in SiO<sub>4</sub> tetrahedra with 4 bridging oxygens),<sup>5,33</sup> and 1110 cm<sup>-1</sup> (combination of P–O stretches of the P–O–P and P–O–Si bridging units),<sup>5,39</sup> Figure 3. At the same time as these bands start to appear, those at ~3400 and 1650 cm<sup>-1</sup> exhibit a reduced intensity while those at 550 and 970 cm<sup>-1</sup> almost disappear, indicating that dehydroxylation reactions occur which progressively transform the dried gels into the phosphosilicate gel-derived glasses. The presence of absorption bands in the 600–800-cm<sup>-1</sup> range for the 30P sample treated at 973–1273 K is indicative of the presence of silicon with 6-fold coordination, related to the crystallization of the 5SiO<sub>2</sub>·3P<sub>2</sub>O<sub>5</sub> phase,<sup>5,20</sup> in agreement with XRD analysis.

On the basis of the above results, the gel-derived glasses heat treated for 1 h at 673 K (SiP-673) were selected for further characterization by solid-state NMR, the characterization of their textural properties as well as the determination of their surface acidity. The importance of the chosen heat treatment is that it represents the minimum required to give a fully inorganic amorphous gel with free phosphoric acid. At higher temperatures, the phosphoric acid reacts substantially with the siloxane matrix, while at lower temperatures, water remains physically trapped in the gel pores as well as organic residuals produced during the chemical processing.

The <sup>29</sup>Si and <sup>31</sup>P MAS NMR spectra are shown in Figures 5 and 6, respectively. Cross linking in the <sup>29</sup>Si NMR spectra can be denoted by the Q<sub>N</sub> notation, where Q<sub>N</sub> indicates Si(OSi)<sub>N</sub>(OX)<sub>4-N</sub>. All the samples regardless of phosphorus content have similar <sup>29</sup>Si NMR spectra with three resonances, at ca. -90, -100, and -110 ppm, in a similar intensity ratio, within experimental error, which can be assigned to Q<sub>2</sub>, Q<sub>3</sub>, and Q<sub>4</sub> structural units, respectively. At first sight, this demonstrates a common siloxane network independent of the phosphorus content. Subtle differences are, however, apparent in the precise chemical shifts for these units which may suggest that some reaction has taken place between the siloxane network and the phosphorus species present. Thus the chemical shift of the Q<sub>4</sub> unit decreases monotonically from -111.1 ppm for 5P-673 to -113.3 ppm for 30P-673. While the -111.1 ppm seen for the Q<sub>4</sub> unit in the 5P-673 is within the normal limits expected for a siloxane network, the value for the 30P-673 lies outside this range in the direction expected for some phosphorus substitution. For

(33) Innocenzi, P. *J. Non-Cryst. Solids* **2003**, 316, 309.

(34) Almeida, R. M.; Guillon, T. A.; Pantano, C. G. *J. Non-Cryst. Solids* **1990**, 121, 193.

(35) Gallardo, J.; Durán, A.; Di Martino, D.; Almeida, R. M. *J. Non-Cryst. Solids* **2002**, 298, 219.

(36) Efimov, A. M. *J. Non-Cryst. Solids* **1997**, 209, 209.

(37) Pawlig, O.; Trettin, R. *Chem. Mater.* **2000**, 12, 1279.

(38) Sunseri, J. D.; Cooper, W. T.; Dorsey, J. G. *J. Chromatogr. A* **2003**, 1011, 23.

(39) Plotnichenko, V. G.; Sokolov, V. O.; Koltashev, V. V.; Dianov, E. M. *J. Non-Cryst. Solids* **2002**, 306, 209.

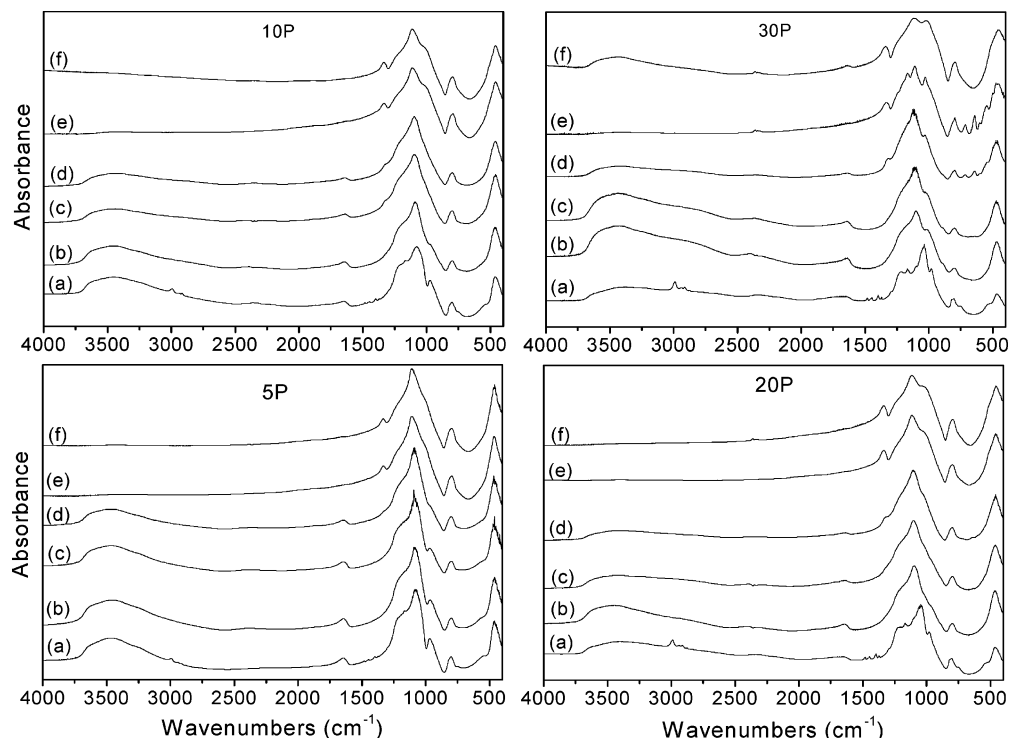


**Figure 3.** FTIR spectra of the studied gels heated at different temperatures: (a) dried gel; (b) 573 K; (c) 1 h at 673 K; (d) 973 K; (e) 1273 K; (f) 1473 K.

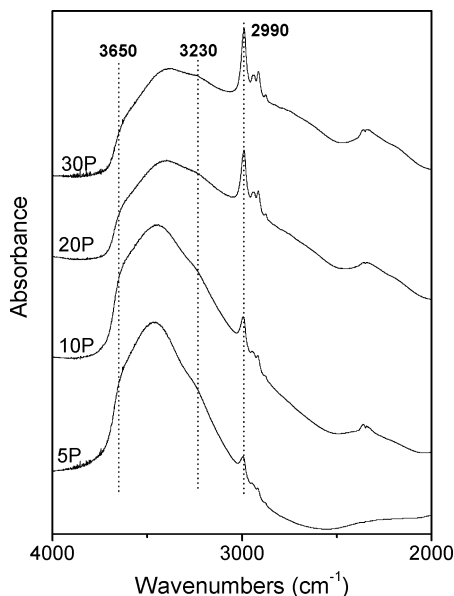


**Figure 4.** FTIR spectra of the dried gels.

example, a fully substituted  $\text{Si}(\text{OP})_4$  unit in  $\text{Si}_5\text{O}(\text{PO}_4)_6$  has a chemical shift of  $-119$  ppm.<sup>10</sup> Discrete resonances for any partially phosphorus-substituted  $\text{Q}_N$  would not be expected given the broad lines of 6–9 ppm at full width at half height, depending on the  $\text{Q}_N$  unit, seen in the  $^{29}\text{Si}$  NMR spectra. Despite the rather weak evidence for the incorporation of phosphorus into the siloxane network, as shown by the small low-frequency shifts, the  $^{29}\text{Si}$  NMR is definitive for the absence of specific amorphous silicon phosphate phases. Thus no evidence is seen for octahedral silicon as would be expected for  $\text{Si}(\text{HPO}_4)_2 \cdot \text{H}_2\text{O}$ <sup>10</sup> or  $\text{Si}_5\text{O}(\text{PO}_4)_6$ .

Turning to the  $^{31}\text{P}$  NMR spectra, these are dominated by an intense resonance at  $-0.08$  ppm, Figure 6. Moreover, despite the solid character of the materials, the narrowness

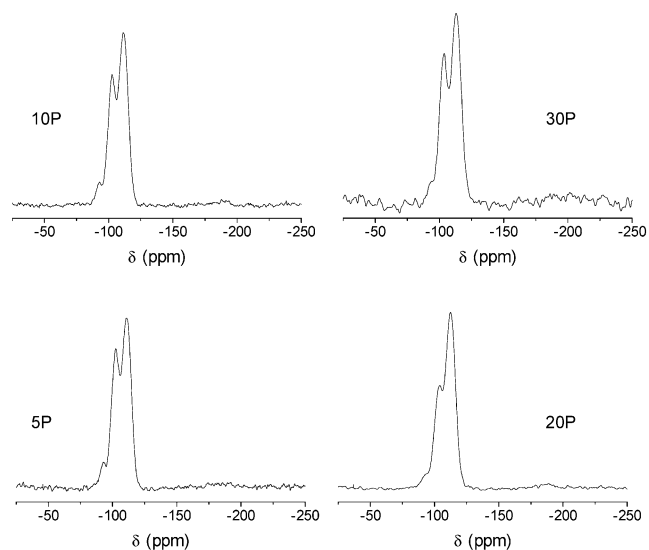


**Figure 5.** 39.7-MHz  $^{29}\text{Si}$  MAS NMR spectra of the SiP samples heated for 1 h at 673 K.

of the  $-0.08$  ppm resonance, and the weak spinning sidebands associated with it, suggest the species giving rise to this resonance is highly mobile. Integration of the  $^{31}\text{P}$  NMR spectra confirms the peak intensities showing that ca. 80% of the phosphorus is present in this form up to and including 20P-673. Only in the case of the 30P-673 sample does the percentage drop significantly, to approximately 47%. Broader resonances are also present in all the  $^{31}\text{P}$  NMR spectra at  $-10.7$  and  $-22.5$  ppm, while the 20P-673 and 30P-673 samples also have a minor resonance at  $-35$  ppm, Figure 6. A resonance at ca. 0 ppm was not observed for silica impregnated using phosphoric acid under anhydrous conditions, though those at  $-10$ ,  $-20$ , and  $-35$  ppm were.<sup>30</sup> On the other hand, when water is not excluded, as in a reaction between  $\text{POCl}_3$  and silica followed by hydrolysis,

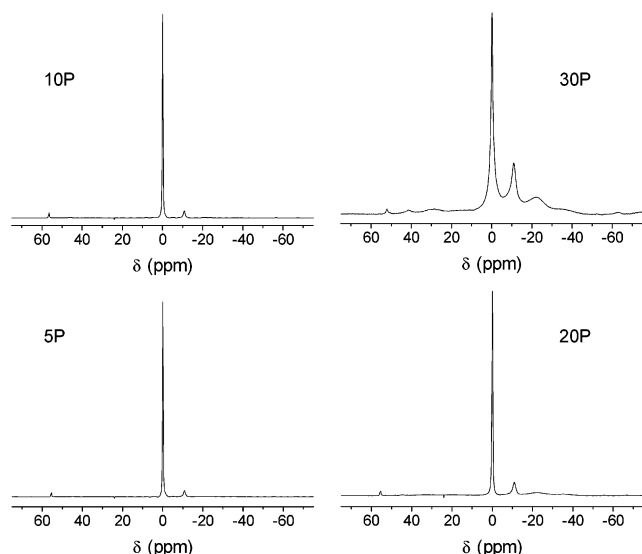


**Figure 6.** 81-MHz  $^{31}\text{P}$  MAS NMR spectra of the SiP samples heated for 1 h at 673 K. The resonances lying outside  $-5$  to  $-50$  ppm are spinning sidebands.

a resonance at ca. 0 ppm was seen along with one at  $-11$  ppm.<sup>31</sup> Yet, in a sequence of water exposure and calcination most similar to those employed for the current materials, namely, an aqueous solution of  $\text{H}_3\text{PO}_4$  followed by calcination at 473 K, again no resonance at 0 ppm was seen.<sup>40</sup> On the basis of the chemical shift alone, it is not possible to identify the  $-0.08$  ppm resonance as being from phosphoric acid, though the chemical shift is consistent with this assignment. In fact, similar to a number of studies of silicas modified using molecular phosphorus precursors, the assignment must be made by a process of elimination: no metal counterions are present to give a metal orthophosphate and silicon orthophosphates all give resonances below  $-30$  ppm.

Uncertainty in the literature exists over the precise assignment of the resonances at  $-10.7$  and  $-22.5$  ppm. On one hand, they have been assigned to terminal and internal groups of phosphoric acid oligomers<sup>10</sup> and on the other hand to phosphorus singly  $\text{SiOP}(\text{O})(\text{OH})_2$  and doubly  $(\text{SiO})_2\text{P}(\text{O})\text{OH}$  bonded to silicon.<sup>31,40</sup> These differences may perhaps be attributed to the different preparative conditions, for when high phosphorus loadings were used with 85% phosphoric acid, diffusion into the bulk of the silica may not occur and the phosphorus would remain concentrated on the external surface allowing dehydration to phosphoric acid oligomers. On the other hand, when solutions of  $\text{H}_3\text{PO}_4$  were used at lower loadings, diffusion into internal surfaces could occur and the phosphorus would be more highly dispersed making cross condensation more likely. In the case of the current materials, clear evidence for cross condensation between the phosphorus and siloxane matrix is provided by the resonance at  $-35$  ppm seen in the  $^{31}\text{P}$  NMR spectra of the 20P-673 and 30P-673 samples. Furthermore, indirect evidence for the assignment of the resonances to a reaction product with the siloxane is provided by  $^{31}\text{P}$  magnetization exchange experiments in phosphosilicate gels prepared by another proce-

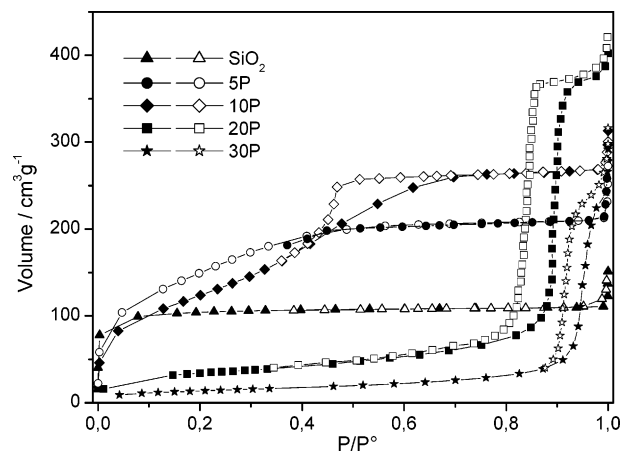


**Figure 7.**  $\text{N}_2$  adsorption-desorption isotherms of  $\text{SiO}_2$  and SiP samples heated for 1 h at 673 K. Full symbols, adsorption; empty symbols, desorption.

dures.<sup>41</sup> At low phosphorus contents, a similar  $^{31}\text{P}$  NMR spectrum to those described here was seen yet no magnetization exchange was observed between resonances at ca.  $-11$  and  $-22$  ppm under conditions in which exchange would be expected if the resonances arose from a polyphosphate. Given the above discussion, the assignment of the  $-10.7$  and  $-22.5$  ppm resonances must remain more tentative than that of the  $-0.08$  ppm resonance. That said, it must be borne in mind that they represent only 20% of the phosphorus in the 5P-673 to 20P-673 samples. Although direct conclusions concerning the absolute dispersion of the phosphorus cannot be made on the basis of the NMR results, it is significant that the vast majority of the phosphorus present is there as an orthophosphate, despite calcination conditions which would favor dehydration to polymerized species. Consequently, it is reasonable to propose the general absence of phosphoric acid oligomers and silicon phosphate phases is because the phosphorus is dispersed more effectively in a siloxane matrix than in other synthetic routes: either sol-gel or impregnation.

#### Textural Properties Characterization.

$\text{N}_2$  adsorption-desorption isotherms for the SiP-673 samples together with the one for a silica gel derived glass heated at 673 K for 1 h (Si-673) are reported in Figure 7. The isotherm for the Si-673 sample shows saturation at low pressure and the absence of any desorption hysteresis as typically occurs in a microporous material. The isotherms for the SiP-673 samples appear quite different from the Si-673 one and depend markedly on composition. Thus, the 5P-673 sample adsorbs more  $\text{N}_2$  than Si-673 and gives an adsorption isotherm with an appreciable gradient over a wide range of  $P/P^0$ . This points to a large contribution of mesopores to the  $\text{N}_2$  adsorption, despite the absence of a desorption hysteresis. The presence of micropores cannot be excluded given the shape of the 5P-673 isotherm. A type IV isotherm, according to the BDDT classification,<sup>28</sup> was seen for the 10P-673 sample together with a higher  $\text{N}_2$  adsorption than the 5P-673 sample for  $P/P^0 > 0.5$ . In addition, a type H2 desorption hysteresis was evident (see

(40) Maki, Y.; Sato, K.; Isobe, A.; Iwasa, N.; Fujita, S.; Shimokawabe, M.; Takezawa, N. *Appl. Catal., A* **1998**, *170*, 269.

(41) Clayden, N. J.; Esposito, S.; Aronne, A. *J. Chem. Soc., Dalton Trans* **2001**, *13*, 2003.



**Table 2. Surface Area, Pore Volume, and Average Pore Radius of Samples Treated at 673 K**

sample	surface area		pore volume (cm <sup>3</sup> g <sup>-1</sup> )	micropore volume (cm <sup>3</sup> g <sup>-1</sup> )	average pore radius <sup>a</sup> <i>r</i> (nm)
	BET (m <sup>2</sup> g <sup>-1</sup> )	$\alpha$ -plot (m <sup>2</sup> g <sup>-1</sup> )			
SiO <sub>2</sub>	313	173	0.17	0.093	1.1
5P	547	445	0.33	0.017	1.2
10P	465	418	0.42		1.8
20P	112	120	0.59		10.5
30P	49	48	0.39		15.9

<sup>a</sup> Average pore radius,  $r = 2V_p/A$ , where  $V_p$  is the pore volume,  $A$  is the BET surface area.

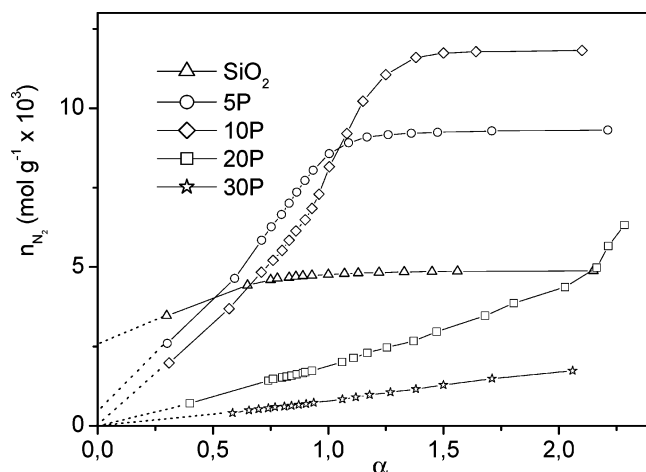
**Figure 8.**  $\alpha$ -Plots of SiO<sub>2</sub> and SiP samples heated for 1 h at 673 K.

Figure 7), characteristic of a material containing pores of different sizes.<sup>28</sup> Markedly different isotherms were obtained for the samples with higher phosphorus concentrations, 20P-673 and 30P-673. In fact they show less-adsorbed N<sub>2</sub> up to  $P/P^0 = 0.8$ – $0.9$ , indeed the very low N<sub>2</sub> adsorption on the sample 30P-673 up to  $P/P^0 = 0.9$  is of particular note, while large gradients are observed when  $P/P^0 > 0.8$ – $0.9$ . Moreover, type H1 hysteresis loops typical of materials containing pores of uniform size<sup>28</sup> were seen for both the 20P-673 and 30P-673 samples.

The N<sub>2</sub> adsorption data of SiP-673 samples have been elaborated by the BET method, and the corresponding surface areas are reported in Table 2. For the Si-673 sample, which is clearly microporous, the BET surface area must be considered a rough approximation. To ascertain the microporous nature of each sample, the  $\alpha$ -plot method has been employed, using the N<sub>2</sub> adsorption isotherm on nonporous silica as a reference.<sup>28</sup> The corresponding curves are reported in Figure 8. Each of the SiP-673 samples gives an  $\alpha$ -plot typical of a mesoporous material, namely, an initial linear branch, followed by an upward deflection caused by capillary condensation in the mesopores, and then a flattened branch, at higher values of  $\alpha$ , that corresponds to saturation of the mesopores with liquid N<sub>2</sub>. This last branch is not visible for the 20P-673 and 30P-673 samples because saturation occurs on these samples at higher  $P/P^0$  values, out of the range of the  $\alpha$ -plot method. On the other hand, in the case of the Si-673 sample, saturation occurs at very low  $\alpha$  values, suggesting the absence of mesopores. In the case of the Si-673 and 5P-673 samples, extrapolation of the  $\alpha$  plots gives positive intercepts, indicating the presence of micropores.<sup>28</sup> The corresponding micropore volumes, calculated assuming

the presence of liquid N<sub>2</sub> in the micropores, are reported in Table 2. On the other hand, for the other SiP-673 samples, the extrapolation of the  $\alpha$  plots pass through the origin, showing the absence of micropores in these samples, Figure 8. The values of the surface area calculated from the  $\alpha$ -plot method are also reported in Table 2 and appear fairly close to those determined by BET with the exception of Si-673 and 5P-673. For these latter samples, the surface areas calculated from  $\alpha$  plots are obviously lower than the “true” ones, because they do not take into account the contribution of the micropores. In Table 2, total pore volumes calculated from the N<sub>2</sub> adsorption at  $P/P^0 = 0.98$  are also reported. These values increase from 0.17 cm<sup>3</sup> g<sup>-1</sup> for pure silica to 0.39 cm<sup>3</sup> g<sup>-1</sup> for the 30P-673 sample going through a maximum for the 20P-673 (0.59 cm<sup>3</sup> g<sup>-1</sup>).

It is well known that the porous properties of dried silica gels are strongly dependent on the conditions used in their synthesis (i.e., monomer concentration, water/alkoxide molar ratio, temperature, and acidity/basicity of the catalyst)<sup>29,42</sup> as well as the presence or otherwise of template molecules.<sup>43–45</sup> In our system, the processing parameters utilized produce a microporous gel-derived silica glass. The textural properties of this material can be compared with those of the silica xerogels obtained by Adeogun and Hay<sup>46</sup> prepared using methanol as the solvent. This comparison shows that the absence of alcohol from the hydrolysis medium allows the preparation of a microporous silica gel derived glass with a high surface area. Furthermore, the above data clearly show that the textural properties of the SiP-673 materials are markedly affected by the P<sub>2</sub>O<sub>5</sub> content. Of particular note, the observed surface areas are much higher than those previously observed for phosphosilicate glasses of similar compositions,<sup>2,23</sup> although, as expected, the values decrease markedly with the phosphorus content. In addition, the morphological features of the siloxane matrix change drastically with increasing phosphorus content. First, the 5P-673 sample shows a small microporous contribution that is absent in the other gel-derived glasses (Figure 8). Second, the 20P-673 and 30P-673 samples have a narrower pore-size distribution with a larger average value (Figure 7, Table 2). A similar trend for the pore-size distribution with the phosphorus content was found by Daiko et al.<sup>2</sup> although these authors related this behavior to the different phosphorus molecular precursors used in the synthesis.

#### Surface Acidity Characterization.

DRIFT and NH<sub>3</sub> TPD spectra were used to characterize the surface acidity. DRIFT spectra of the SiP-673 samples in the spectral range 4000–2000 cm<sup>-1</sup> are shown in Figure 9, together with a reference spectrum of Si-673. The spectrum of Si-673 shows a sharp feature at 3650 cm<sup>-1</sup>, which can be assigned to free SiOH groups and a broad band at 3700–2800 cm<sup>-1</sup>, arising from OH groups engaged in hydrogen

(42) Fidalgo, A.; Rosa, M. E.; Ilharco, L. M. *Chem. Mater.* **2003**, *15*, 2186.

(43) Lu, Y.; Cao, G.; Kale, R. P.; Prabakar, S.; L pez, G. P.; Brinker, C. J. *Chem. Mater.* **1999**, *11*, 1223.

(44) Scott, B. J.; Wirmsberger, G.; Stucky, G. D. *Chem. Mater.* **2001**, *13*, 3140.

(45) Takahashi, R.; Sato, S.; Sodesawa, T.; Kawakita, M.; Ogura, K. J. *Phys. Chem. B* **2000**, *104*, 12184.

(46) Adeogun, M. J.; Hay, J. N. *Chem. Mater.* **2000**, *12*, 767.



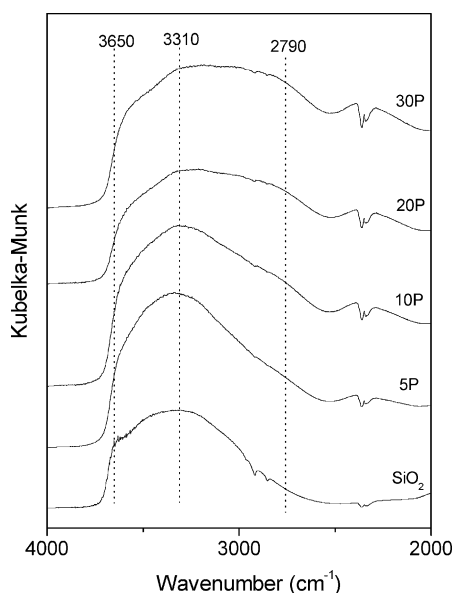


**Figure 9.** DRIFT spectra of SiO<sub>2</sub> and SiP samples heated for 1 h at 673 K.

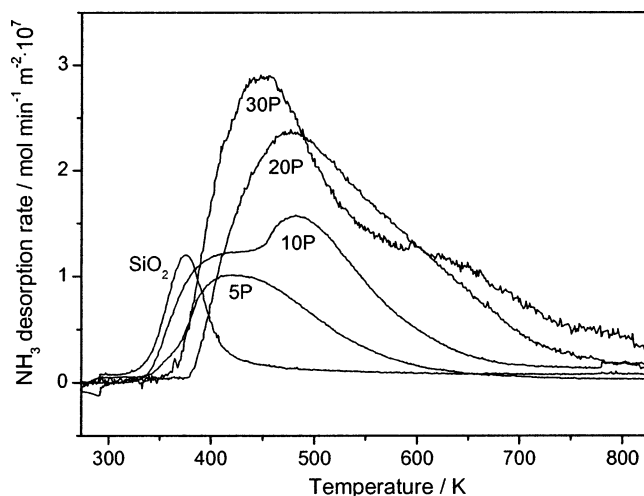


**Figure 10.** NH<sub>3</sub> TPD spectra of SiO<sub>2</sub> and SiP samples heated for 1 h at 673 K.

bonds of moderate strength. Thus, as expected, Si-673 contains free silanols groups and silanol hydrogen bonded to water molecules or to the siloxane framework. Broadly speaking, the DRIFT spectra of the phosphosilicate samples are similar to those of the corresponding transmission spectra (Figure 4), although the differences among the samples appear enhanced. All samples show a broad band in the range 3700–2500 cm<sup>-1</sup>, with a sharper component at about 3650 cm<sup>-1</sup>. As discussed above, the broad band mainly arises from the PO–H stretch of groups involved in hydrogen bonds. Increasing phosphorus content leads to a shoulder at about 2790 cm<sup>-1</sup>, showing that this causes an increase of the strength of H bonding as well as of the acid strength of POH groups.<sup>47</sup>

NH<sub>3</sub> TPD profiles of the Si-673 and SiP-673 samples are shown in Figure 10. Integration of the area underlying the TPD peaks yields the amount of adsorbed NH<sub>3</sub> as reported

**Table 3.** Adsorbed NH<sub>3</sub> Amounts from TPD Measurements of Samples Treated at 673 K

sample	adsorbed NH <sub>3</sub>		NH <sub>3</sub> /P mol mol <sup>-1</sup>
	(mmol g <sup>-1</sup> )	(molecule nm <sup>-2</sup> )	
SiO <sub>2</sub>	0.20	0.38	
5P	0.76	0.84	0.49
10P	1.20	1.55	0.50
20P	0.51	2.74	0.15
30P	0.23	2.85	0.044

in Table 3. These values correspond to the concentrations of acid sites by assuming a stoichiometric acid site:NH<sub>3</sub> ratio equal to 1:1. A striking variation is seen depending on the phosphorus content of the sample. The profile for Si-673 consists of a single symmetric peak at low temperature, indicating the presence of weak acid sites of a homogeneous type. On the other hand, all the SiP samples show profiles typical of a distribution of acid sites together with a greater number of sites and increased acid strength. Thus, for 5P-673, a broad and tailed peak is obtained, with a predominance of medium strength acid sites. This effect is even more marked with the sample 10P-673, showing a large composite TPD signal, in which two peaks are recognizable and a long tail at high temperature. Compared with 5P-673, 10P-673 therefore has a wider distribution of acid strengths and the likely presence of two types of acid sites. At higher P<sub>2</sub>O<sub>5</sub> contents for 20P-673, the TPD curve broadens and increases in intensity further, with a tail extending to higher temperatures, pointing to a more heterogeneous acidity and a greater surface concentration of acid sites. Similarly, a large and broad signal with a long tail is observed for 30P-673, though in this case a high-temperature signal is also clearly evident. As shown in Table 3, the concentration of acid sites per unit mass reaches a maximum with 10P-673, while the concentration of acidity per unit surface increases with P<sub>2</sub>O<sub>5</sub> content up to the 30P-673 sample. Also of note, the ratio NH<sub>3</sub>/P is always less than 0.5 and decreases with increasing phosphorus content.

The above data show that the acidity of the SiP-673 samples is greatly influenced by their composition. In agreement with previous studies, the pure silica sample exhibits a limited number of weak acid sites, corresponding to SiOH groups.<sup>48–49</sup> On the other hand, the SiP-673 samples contain acid sites of greater strength attributable to the presence of phosphoric acid with evidence from the shapes of the TPD curves for at least two types of sites: this is particularly true for the 10P-673 sample but can also be seen in the curves for the other samples. Moreover, the strong acid sites, that is, those releasing NH<sub>3</sub> at  $T > 673$  K, increase with P<sub>2</sub>O<sub>5</sub> content. Different types of POH groups with varying acid strengths have been seen previously by Busca et al.<sup>47</sup> in SiO<sub>2</sub> impregnated with H<sub>3</sub>PO<sub>4</sub>.

Thus DRIFT spectra and NH<sub>3</sub> TPD agree that the acid strength increases with P<sub>2</sub>O<sub>5</sub> content. A structural model consistent with this behavior as well as the NMR evidence is to consider the SiP-673 samples as having a siloxane

(47) Busca, G.; Ramis, G.; Lorenzelli, V.; Rossi, P. F.; La Ginestra, A.; Patrono, P. *Langmuir* **1989**, 5, 911.

(48) Auroux, A.; Monaci, R.; Rombi, E.; Solinas, V.; Sorrentino, A.; Santacesaria, E. *Thermochim. Acta* **2001**, 379, 227.

(49) Kostova, N. G.; Spojakina, A. A.; Jiratova, K.; Solcova, O.; Dimitrov, L. D.; Petrov, L. A. *Catal. Today* **2001**, 65, 217.

framework covered to a greater or lesser extent by molecular phosphoric acid. When the P content is low, a monolayer of  $\text{H}_3\text{PO}_4$  will be formed, with the  $\text{H}_3\text{PO}_4$  molecules strongly interacting with the siloxane matrix, mainly through H-bridges with O atoms. On the other hand, when the P content is high, several  $\text{H}_3\text{PO}_4$  layers are present around the siloxane framework and most  $\text{H}_3\text{PO}_4$  molecules interact with other  $\text{H}_3\text{PO}_4$  molecules rather than with silica. It is expected that these differing conditions influence the strength of the acid sites, since  $\text{H}_3\text{PO}_4$  should be more acidic when bonded to other  $\text{H}_3\text{PO}_4$  molecules than when bonded to the siloxane matrix, owing to the higher electronegativity of phosphorus compared to that of silicon. To account for the fact that a monolayer coverage of  $\text{H}_3\text{PO}_4$  corresponds to a concentration of  $6.7 \mu\text{mol m}^{-2}$ ,<sup>47</sup> the  $\text{H}_3\text{PO}_4$  content, based on the composition and surface area, is well below the value required to give monolayer coverage for the 5P and 10P samples (41 and 72%, respectively), while for the 20P and 30P samples, it greatly exceeds the monolayer value (420 and 1400%). Consequently a general increase of acid strength with phosphorus content is expected, especially when going from 10P to 20P samples, in agreement with DRIFT and  $\text{NH}_3$  TPD data.

One further feature of the  $\text{NH}_3$  TPD data is that the amount of desorbed  $\text{NH}_3$  was always much lower than the value expected on the basis of each  $\text{H}_3\text{PO}_4$  molecule giving at least one proton. From Table 3, it is seen that even when the  $\text{H}_3\text{PO}_4$  can be expected to be well dispersed, as is the case for the high surface area 5P-673 and 10P-673, the  $\text{NH}_3/\text{P}$  ratio is only 0.5, suggesting that half of the  $\text{H}_3\text{PO}_4$  molecules are not available for a reaction with  $\text{NH}_3$ . A similar behavior was found for a material containing a monolayer of  $\text{H}_3\text{PO}_4$  spread on  $\text{SiO}_2$ , obtained by impregnation.<sup>50</sup> Possible explanations for this result are that either the  $\text{H}_3\text{PO}_4$  molecules

are not evenly spread around the siloxane chains or a fraction of these molecules have reacted with silanol groups during the treatment at 673 K. In the former case, a multilayer would exist, even in 5P and 10P samples, so that the acid is only partly exposed on the surface and thus able to react with the base. In the latter case, the number of POH groups would have been reduced by the condensation of some of them with SiOH groups, to form Si—O—P bonds, but this hypothesis appears unlikely on the basis of the NMR results.

## Conclusions

A new sol-gel method has been used successfully to prepare phosphosilicate glasses. Hydrolysis of the molecular precursors in almost purely aqueous solutions has been shown to increase the gelation rate, to facilitate the removal of the solvent, and to permit a high dispersion of phosphorus in the siloxane matrix. In addition, the heat-treated materials remain amorphous over a wide temperature range, showing a low tendency toward crystallization. Higher surface areas are found in comparison with similar phosphosilicate glasses described in the literature. The strong influence of the Si/P ratio on the surface area and pore size, that was only suspected from previous work, has been clearly shown. Moreover, it has been found that surface acidity is also strongly dependent on the composition.

The synthesized materials could be employed as catalysts or gas sensors because of their interesting physical and chemical properties.

**Acknowledgment.** This work was supported by Italian Ministry of Education, University and Research, COFIN 2002, Prot. 2002095575-003.

CM047768T

(50) Ramis, G.; Rossi, P. F.; Busca, G.; Lorenzelli, V.; La Ginestra, A.; Patrono, P. *Langmuir* **1989**, *5*, 917.